

Optimizing Utility-Energy Efficiency for the Metaverse over Wireless Networks under Physical Layer Security

Jun Zhao, Xinyu Zhou, Yang Li, Liangxin Qian

Nanyang Technological University, Singapore

junzhao@ntu.edu.sg, {xinyu003, yang048, qian0080}@e.ntu.edu.sg

ABSTRACT

The Metaverse, an emerging digital space, is expected to offer various services mirroring the real world. Wireless communications for mobile Metaverse users should be tailored to meet the following user characteristics: 1) emphasizing application-specific utility instead of simply the transmission rate, 2) concerned with energy efficiency due to the limited device battery and energy-intensiveness of some applications, and 3) caring about security as the applications may involve sensitive personal data. To this end, this paper incorporates application-specific utility, energy efficiency, and physical-layer security (PLS) into the studied optimization in a wireless network for the Metaverse. Specifically, after introducing utility-energy efficiency (UEE) to represent each Metaverse user's application-specific objective under PLS, we formulate an optimization to maximize the network's weighted sum-UEE by deciding users' transmission powers and communication bandwidths. The formulated problem belongs to the sum-of-ratios optimization, for which prior studies have demonstrated its difficulty. Nevertheless, our proposed algorithm 1) obtains the global optimum for the optimization problem, via a transform to parametric convex optimization problems, 2) applies to any utility function which is concave, increasing, and twice differentiable, and 3) achieves a linear time complexity in the number of users (the optimal complexity in the order sense). Simulations confirm the superiority of our algorithm over other approaches. We envision that our technique for solving the challenging sum-of-ratios optimization can be applied to other optimization problems in wireless networks and mobile computing.

KEYWORDS

Wireless networks, Metaverse, physical layer security, resource allocation, utility-energy efficiency.

1 INTRODUCTION

The Metaverse [1] is considered as the next generation of the Internet, which consolidates virtual reality/augmented reality (VR/AR), 3D technologies, etc. The Metaverse will provide digital services which may interact with the physical world. In 2021, Facebook changed its name to Meta, raising public interest in the Metaverse.

Permission to make digital or hard copies of all or part of this work for personal or classroom use is granted without fee provided that copies are not made or distributed for profit or commercial advantage and that copies bear this notice and the full citation on the first page. Copyrights for components of this work owned by others than ACM must be honored. Abstracting with credit is permitted. To copy otherwise, or republish, to post on servers or to redistribute to lists, requires prior specific permission and/or a fee. Request permissions from permissions@acm.org.
Conference'23, 2023, Washington, DC, USA

© 2023 Association for Computing Machinery.
ACM ISBN 978-1-4503-XXXX-X/18/06...\$15.00
<https://doi.org/XXXXXXX.XXXXXXX>

Characteristics of Metaverse users. We identify the following traits for mobile users of the Metaverse.

- ① Users aim to maximize **application-specific utility** rather than simply the transmission rate. Traditional network optimization considers the Quality of Service (QoS), which captures the physical performance of the system. An example QoS metric is the transmission rate. For the Metaverse, the Quality of Experience (QoE) captures the actual experience of users and thus is more important than the QoS. The QoE depend on specific applications.
- ② Users care about **energy efficiency** due to the limited battery of mobile devices and energy-intensiveness of some applications. For instance, Meta Oculus Quest 2 with fully charged battery can last for just 2 hours for gaming or 3 hours for video watching [2].
- ③ Users are concerned with **security** since certain Metaverse applications may involve personal (e.g., biometric and health) data. Researchers at UC Berkeley have shown in [3] that many existing Metaverse applications are vulnerable to privacy breach by an attacker which tries to infer users' sensitive information.

The Metaverse over wireless networks: Utility-energy efficiency optimization under physical-layer security. Since mobile users accessing the Metaverse are constrained by wireless communication resources, it is important to tailor wireless communications to meet the above characteristics of Metaverse users. We formalize the problem as an optimization about the utility-energy efficiency (UEE) under physical-layer security, where UEE for each user is defined as the utility over transmission energy consumption, for the motivation discussed below.

Energy efficiency plays a vital role in both the economy and the environment. Faster transmission rate providing higher quality of experience for users will also increase the energy consumption. Therefore, it is essential to build an energy-efficient Metaverse system. Nevertheless, it is not viable to emphasize energy saving overwhelmingly. The Metaverse covers all aspects of life, and lower transmission speeds will affect users' access to profits and high-quality experience. Hence, how to allocate the resources (e.g., the transmission power and bandwidth) for the whole system to maximize the weighted sum of all users' UEE is worth investigating, where each user's weight represents its priority in the system optimization. The weighted sum-UEE optimization aims to save energy and improve the utilities for users, addressing "①" and "②" above.

For "③" above, the confidential data of Metaverse applications should be accessible to only the intended users instead of eavesdroppers. To this end, we aim to achieve physical-layer security to protect the information during transmission. Secrecy capacity is one of the physical-layer security methods. It refers to the communication rate that does not leak information to an eavesdropper. It

is subject to the signal-to-noise ratio (SNR) of the legitimate channel being larger than the eavesdropper's channel. In order to keep the information of users from the eavesdroppers, we extend our Metaverse energy efficiency problem to the physical-layer security by incorporating the secrecy rate into the objective function.

Challenges. Different from ordinary VR/AR applications nowadays, Metaverse stresses immersive experience and immediate feedbacks. To fulfill the Metaverse world, several challenges remained to be tackled: 1) Current computation and communication resources cannot meet the Metaverse's requirements for low latency and high bandwidth. 2) Data security and user privacy are also critical aspects to the Metaverse world. 3) If users are immersed in the Metaverse, their experience will be affected by the transmission rate since it is apparent that the faster the transmission rate, the greater the gain based on different utility function. Hence, how to efficiently utilize limited resources while protecting the physical-layer security is worth investigating.

In this paper, we introduce the physical-layer security into the Metaverse energy efficiency problem and solve it by allocating the transmission power and bandwidth for each user appropriately. However, this problem is a sum-of-ratios problem, which is non-convex and difficult to solve.

Contributions. Our contributions are listed as follows:

- We investigate utility-energy efficiency, which is defined as the achieved utility when consuming a unit of power in Metaverse. It is a generalization of the traditional energy efficiency.
- Our problem is applicable to both downlink and uplink communications.
- Our proposed **algorithm**
 - obtains the **global optimum** for the weighted sum-UEE optimization problem, via a transform to parametric convex optimization problems,
 - applies to **any** utility function which is concave, increasing, and twice differentiable, and
 - allows **heterogeneous** types of utility functions among the users,
 - runs in **linear** time with respect to the number of users, which means the **optimal complexity** in the order sense.
- Simulations demonstrate the superiority of our algorithm over other approaches in terms of the solution quality and time complexity. The utility functions used in the simulations are also confirmed by experiments with **real data**.
- We abstract our algorithm into a useful **technique** which can handle functions of product or quotient terms in optimization problems. We also point out that the presented technique is applicable to other optimization problems in wireless networks and mobile computing.

Roadmap. The rest of the paper is organized as follows. Section 2 provides related studies. In Section 3, we formulate the studied optimization problem. Section 4 presents the challenges in solving the problem. Section 5 elaborates on our algorithm which finds a global optimum of the problem. In Section 6, we discuss the insights from our optimization technique with applications to other problems in wireless networks and mobile computing. Numerical results are reported in Section 7. Finally, Section 8 concludes the paper.

2 RELATED WORK

In this section, we survey related research. Section 2.1 is devoted to the optimization of energy efficiency and related metrics in wireless networks. Section 2.2 illustrates the Metaverse over wireless networks, which is our main application scenario. Section 2.3, we elaborate physical-layer security, another key factor to consider in the communication process of the Metaverse.

2.1 Optimization of energy efficiency and related metrics in wireless networks

Huang *et al.* [4] introduced the concept of utility-energy efficiency (UEE), which for each user is defined as the ratio of a rate-functioned utility over the power consumption, the same way as in our paper. However, one major limitation of [4] is that their optimization method is applicable to only the specific utility function $\kappa_n \ln r_n$ for data rate r_n and constant κ_n . Even just changing the utility function to $\kappa_n \ln(1 + r_n)$ will make their approach invalid; in particular, (18a) in [4] will be non-convex after the above change. In contrast, our work applies to any utility function that is concave, increasing, and twice differentiable. In addition to the major distinction above, another difference between [4] and our work is that [4] considers interference-constrained wireless networks and optimizes only the transmission powers, while we adopt FDMA and jointly optimize the transmission powers and bandwidth allocation.

There are also some other studies about the optimization of energy efficiency and wireless networks [5, 6]. For example, [5] solved the maximization problem of the secure energy efficiency, which is defined as the secrecy rate divided by power consumption, to allocate the source and relay power. [6] researched optimum energy efficiency and the corresponding spectral efficiency over a flat-fading channel under different cases and developed a polynomial-complexity algorithm to balance them.

2.2 Metaverse over wireless networks

Metaverse is a virtual world that based on numerous technologies, one of the most important of which is wireless communication system. The development of wireless networks has laid a solid foundation for the integration of virtual reality (VR), augmented reality (AR), mixed reality (MR), digital twin (DT) and so on, which are key components of the Metaverse. An adaptive VR framework that enables high-quality wireless VR in future mmWave-enabled wireless networks with mobile edge computing (MEC) was proposed by [7], where real-time VR rendering tasks can be offloaded to MEC servers adaptively and the caching capability of MEC servers enables further performance improvement.

In wireless systems, the Metaverse has two main aspects: offline analysis and online control. The former can guide us regarding design and deployment of wireless systems. An analysis of this type can be performed using various simulation tools a priori (e.g., for system level simulation, signal processing, network protocols, and routing, and mobility simulations). Besides analyzing virtual wireless worlds, one can control physical systems in the Metaverse at run-time. Further, wireless communications and networking can be used in conjunction with other technologies (e.g., blockchain and edge computing) to allow seamless interaction between the virtual and physical worlds.

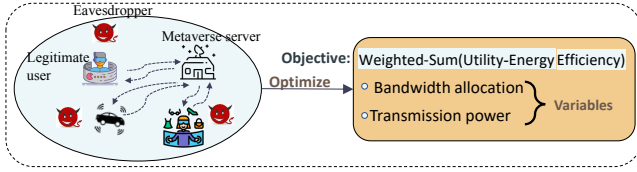


Figure 1: Our system: A server provides Metaverse services for N legitimate users $U_n|_{n=1,\dots,N}$, while the n th eavesdropper E_n tries to intercept the communication between user U_n and the server. The studied problem is to maximize the weighted sum of all users' utility-energy efficiency by deciding the bandwidth allocation and transmit power.

2.3 Physical-layer security

Initially, physical-layer security was developed by defining a wiretap channel's secrecy capacity in [8] and [9]. This capacity defines the upper bound of all achievable secrecy rates. Recent studies on physical-layer security can be roughly summarized from two main aspects: 1) the studies related to system designs from the viewpoints of optimization and signal processing 2) And the studies related to secrecy rate/capacity from the perspective of information-theoretic security. The first aspect mainly focuses on the secure strategy designs based on the techniques of optimization and signal processing. On the other hand, the second aspect mainly focuses on the secrecy capacity, achievable secrecy rate, and capacity-equivocation region based on the ideas of information theory.

Secure system design: [10] provided results in information-theoretic security with multiple wireless transmitters, and focuses on distilling insights for designing wireless systems with confidentiality guarantees. Subcarrier allocation problem of secure

Secrecy Rate/Capacity: [11] defined secrecy capacity in wireless channels and provided a complete characterization of the maximum transmission rate.

3 PROBLEM FORMULATION

In this section, we will present the system model and formalize the optimization problem.

3.1 System model and metrics

In our studied system, a base station acts as the Metaverse server for N legitimate users $U_n|_{n=1,\dots,N}$. There are also N eavesdroppers $E_n|_{n=1,\dots,N}$, where the eavesdropper E_n tries to intercept the communication between legitimate user U_n and the Metaverse server (abbreviated as "the server" sometimes). Fig. 1 illustrates our system.

We consider that communications between all legitimate users and the Metaverse server follow frequency division multiple access (FDMA). With FDMA, different legitimate users' signals will not interfere with each other. For each legitimate user U_n , let p_n be its transmission power and B_n be the bandwidth, for uplink communication with the Metaverse server. Throughout this paper, the n th dimension of an N -dimensional vector \mathbf{x} is denoted by x_n (unless stated otherwise); i.e., $\mathbf{x} = [x_n]_{n \in \mathcal{N}}$ for $\mathcal{N} := \{1, \dots, N\}$. Hence, we have $\mathbf{p} := [p_1, p_2, \dots, p_N]$ and $\mathbf{B} := [B_1, B_2, \dots, B_N]$.

Transmission rate. We consider the uplink communication from users to the Metaverse server. According to the Shannon

formula, the transmission rate $r_n(p_n, B_n)$ of legitimate user U_n is

$$r_n(p_n, B_n) = B_n \log_2 \left(1 + \frac{g_n p_n}{\sigma_n^2 B_n} \right), \quad (1)$$

where B_n is the bandwidth allocated to user U_n , σ_n^2 is the power spectral density of Gaussian noise, g_n is the channel attenuation from user U_n to the server. Note that the function notation is used throughout this paper; e.g., $r_n(p_n, B_n)$ is a function of p_n and B_n .

Secrecy rate. The eavesdropper E_n aims to intercept the communication between legitimate user U_n and the server. Let $r_{n,e}$ be the eavesdropping rate of E_n . In this paper, we consider $r_{n,e}$ as a constant depending on only n . Then the secrecy rate of legitimate user U_n is given by

$$r_{n,s}(p_n, B_n) := r_n(p_n, B_n) - r_{n,e}. \quad (2)$$

Utility. We consider user U_n 's utility rate as a function of the secrecy rate $r_{n,s}(p_n, B_n)$ to emphasize physical-layer security. Specifically, using¹ $f_n(\cdot) : (0, \infty) \rightarrow (-\infty, \infty)$ to denote the utility rate function, user U_n 's utility rate is given by $f_n(r_{n,s}(p_n, B_n))$. Consider a small time interval $[t, t + \Delta t]$, where Δt is small enough such that $r_{n,s}(p_n, B_n)$ can be considered as invariant during $[t, t + \Delta t]$. Then the utility of user U_n over the time interval $[t, t + \Delta t]$ is $\mathcal{U}_n^{[t, t + \Delta t]} := f_n(r_{n,s}(p_n, B_n)) \Delta t$.

Power & energy consumption. The same as [4, 12], the power consumed by user U_n includes not just the transmission power p_n , but also the circuit power p_n^{cir} . We consider p_n^{cir} to be a constant given n , denoting the circuit power [12]. During the time interval $[t, t + \Delta t]$, user U_n 's energy consumption is given by $\mathcal{E}_n^{[t, t + \Delta t]} := (p_n + p_n^{\text{cir}}) \Delta t$.

Utility-energy efficiency. For user U_n , we define its utility-energy efficiency (UEE) $\varphi_n(p_n, B_n)$ at time t as the ratio of $\frac{\mathcal{U}_n^{[t, t + \Delta t]}}{\mathcal{E}_n^{[t, t + \Delta t]}}$ for small enough Δt , which induces²

$$\varphi_n(p_n, B_n) := \frac{f_n(r_{n,s}(p_n, B_n))}{p_n + p_n^{\text{cir}}} = \frac{f_n(r_n(p_n, B_n) - r_{n,e})}{p_n + p_n^{\text{cir}}}. \quad (3)$$

When $f_n(\cdot)$ becomes the identity function (i.e., $f_n(x) = x$), $\varphi_n(p_n, B_n)$ becomes $\frac{r_{n,s}(p_n, B_n)}{p_n + p_n^{\text{cir}}}$ (i.e., $\frac{\text{secrecy rate}}{\text{power consumption}}$), which is just the traditional notion of energy efficiency under physical-layer security [13].

3.2 Utility-energy efficiency (UEE) optimization

Our goal is to maximize the weighted sum of all users' UEE. This optimization problem is formalized as follows:

$$\text{Problem } \mathbb{P}_1: \max_{\mathbf{p}, \mathbf{B}} \sum_{n \in \mathcal{N}} c_n \varphi_n(p_n, B_n) \quad (4)$$

$$\text{subject to: } \sum_{n \in \mathcal{N}} B_n \leq B_{\text{total}}, \quad (4a)$$

$$r_n(p_n, B_n) \geq r_n^{\min}, \text{ for all } n \in \mathcal{N}. \quad (4b)$$

¹We require $f_n(x)$ to be defined for any $x > 0$. We do not require $f_n(x)$ to be defined for $x = 0$, but if $\lim_{x \rightarrow 0^+} f_n(x)$ exists and is finite, we can just use it to define $f_n(0)$. We also do not enforce any condition on whether $f_n(x)$ is non-negative or not. Additional conditions of $f_n(x)$ are discussed in Section 4.2.

²Although we place our studied problem in the context of uplink communications from legitimate users to the Metaverse server. Our problem can also apply to downlink communications from the server to legitimate users. For downlink communications, the circuit power p_n^{cir} in the denominator $p_n + p_n^{\text{cir}}$ of (3) is the additional power that the server consumes to transmit signals with power p_n to user U_n , and it is possible that p_n^{cir} can be the same for different n for such downlink communications.

where $c_n > 0$ represents the priority of user U_n in our UEE optimization. Larger c_n means higher priority. Constraints (4a) sets the total bandwidth for FDMA. Constraint (4b) ensures that the transmission rate $r_n(p_n, B_n)$ of user U_n should be at least a constant r_n^{\min} (r_n^{\min} can vary for different n). Condition 1 below is about minimum legitimate rates $r_n^{\min}|_{n \in \mathcal{N}}$ and eavesdropping rates $r_{n,e}|_{n \in \mathcal{N}}$.

CONDITION 1. For all $n \in \mathcal{N}$, we have $r_n^{\min} \geq r_{n,e}$, $r_n^{\min} > 0$, $r_{n,e} \geq 0$.

We have the following remarks about Condition 1.

REMARK 1. Condition 1 with (4b) ensures $r_n(p_n, B_n) \geq r_{n,e}$; i.e., each user U_n 's secrecy rate $r_{n,s}(p_n, B_n)$ is non-negative.

REMARK 2. Condition 1 covers the following special case where we do not consider physical-layer security but still enforce a minimum transmission rate for each user: $r_{n,e} = 0$ and $r_n^{\min} > 0$ for all $n \in \mathcal{N}$.

REMARK 3. We enforce $r_n^{\min} > 0$ in Condition 1 so that each user U_n will always be allocated with a strictly positive bandwidth. This avoids analyzing the degenerate case where only a subset of \mathcal{N} users share the total bandwidth B_{total} .

We also comment on how Problem \mathbb{P}_1 is optimized in practice.

REMARK 4. Problem \mathbb{P}_1 will be solved using our Algorithm 1 in Section 5.2. Then a question is which entity solves \mathbb{P}_1 in practice. We let the Metaverse server perform the task, assuming that it has obtained the values of p_n^{cir} , r_n^{\min} , $r_{n,e}$ for all n (e.g., these are shared with the server before the optimization stage). After the server solves \mathbb{P}_1 , it will notify each legitimate user U_n of the p_n and B_n values.

4 CHALLENGES IN SOLVING PROBLEM \mathbb{P}_1 DUE TO NON-CONVEX OPTIMIZATION

4.1 Preliminaries

Let $f(\mathbf{x})$ be a function defined on a convex set \mathcal{S} , which is a subset of a real vector space. Then we have the following from Definitions 1.3.1, 2.2.1, and 3.2.1 of the book [14].

DEFINITION 1 (CONVEXITY). f is convex in \mathbf{x} if and only if for any $\mathbf{x}_1, \mathbf{x}_2 \in \mathcal{S}$ and $t \in [0, 1]$, it holds that $f(t\mathbf{x}_1 + (1-t)\mathbf{x}_2) \leq tf(\mathbf{x}_1) + (1-t)f(\mathbf{x}_2)$.

DEFINITION 2 (PSEUDOCONVEXITY). f is pseudoconvex in \mathbf{x} if and only if for any $\mathbf{x}_1, \mathbf{x}_2 \in \mathcal{S}$, $f(\mathbf{x}_1) > f(\mathbf{x}_2)$ implies $\nabla f(\mathbf{x}_1) \cdot (\mathbf{x}_2 - \mathbf{x}_1) < 0$, where ∇f denotes the gradient of f .

DEFINITION 3 (QUASICONVEXITY). f is quasiconvex in \mathbf{x} if and only if for any $\mathbf{x}_1, \mathbf{x}_2 \in \mathcal{S}$ and $t \in [0, 1]$, it holds that $f(t\mathbf{x}_1 + (1-t)\mathbf{x}_2) \leq \max\{f(\mathbf{x}_1), f(\mathbf{x}_2)\}$.

With convexity above, Lemma 4.1 helps us understand concavity.

LEMMA 4.1 (CONVEXITY VS CONCAVITY). A function f is said to be concave (resp., pseudoconcave, quasiconcave) if and only if $-f$ is convex (resp., pseudoconvex, quasiconvex).

For the reasoning behind Lemma 4.1, interested readers can refer to Section 3 of the book [14]. Lemma 4.2 below presents the relationships between the definitions discussed above.

LEMMA 4.2 (RELATIONSHIPS BETWEEN NOTIONS). With “ \Rightarrow ” denoting “implies”, we have the following assuming differentiability
Convexity \Rightarrow Pseudoconvexity \Rightarrow Quasiconvexity, and (5)

$$\text{Concavity} \Rightarrow \text{Pseudoconcavity} \Rightarrow \text{Quasiconcavity}. \quad (6)$$

Lemma 4.2 follows from Fig. 2.2 and Fig. B.1 of the book [14].

With the above definitions and lemmas, we now discuss the properties of functions in our studied system.

LEMMA 4.3 (LEMMA 1 OF [15]). $r_n(p_n, B_n)$ is jointly concave with³ respect to p_n and B_n .

LEMMA 4.4. Suppose that the utility rate function $f_n(x)$ for any $n \in \mathcal{N}$ is increasing and concave for $x > 0$ (to be elaborated in Section 4.2). Then we have:

- $f_n(r_{n,s}(p_n, B_n))$ is jointly concave with respect to p_n and B_n ;
- $\varphi_n(p_n, B_n)$ is jointly pseudoconcave with respect to p_n and B_n .

PROOF. From Lemma 4.3 and Eq. (2), $r_{n,s}(p_n, B_n)$ is jointly concave with respect to p_n and B_n . Then according to the composition rule in Eq. (3.10) of [16], for concave and increasing $f_n(\cdot)$, the function $f_n(r_{n,s}(p_n, B_n))$ is jointly concave with respect to p_n and B_n .

In $\varphi_n(p_n, B_n)$, the numerator $f_n(r_{n,s}(p_n, B_n))$ is concave as just proved, while the denominator $p_n + p_n^{\text{cir}}$ is affine (i.e., both convex and concave). From Page 245 (the book's internal page number, not the pdf page number) of the book [14], for a ratio, if the numerator is non-negative, concave and differentiable, and the denominator is positive, convex and differentiable, then the ratio is pseudoconcave. Based on the above, we have proved the pseudoconcavity of $\varphi_n(p_n, B_n)$ with respect to p_n and B_n . \square

For a minimization problem, if the objective function and⁴ the constraints are all convex, then we have a convex optimization problem, for which the following lemma holds.

LEMMA 4.5 (CHAPTERS 3 AND 4 OF [16]). For convex optimization, the Karush–Kuhn–Tucker (KKT) conditions are

- sufficient for optimality, and
- are necessary for optimality if Slater's condition holds (i.e., if the feasible set contains at least one interior point).

Readers unfamiliar with the KKT conditions can refer to Theorem 4.2.3 of [14]. Readers can also look into (14a)–(14l) to be presented on Page 6 of the current paper, where we will use the KKT conditions.

Lemma 4.6 below broadens problems under which KKT conditions are sufficient for optimality, to go beyond convex optimization.

LEMMA 4.6 (THEOREM 4.4.1 OF [14]). For a minimization problem with all constraints being inequalities, if the objective function is pseudoconvex, and all constraints are quasiconvex and differentiable, then a feasible point satisfying the KKT conditions is globally optimal.

4.2 Conditions of the utility function $f_n(x)$

The requirements of the utility rate function $f_n(x)$ for any $n \in \mathcal{N}$ are formally presented as Condition 2 below (we will just call $f_n(x)$ as the utility function hereafter for simplicity).

CONDITION 2. The utility function $f_n(x)$ for any $n \in \mathcal{N}$ is concave, increasing, and twice differentiable, with respect to $x > 0$; i.e., $f_n''(x) \leq 0$ and $f_n'(x) > 0$ for $x > 0$.

³For a function $f(\mathbf{x})$, “being convex (resp., concave) in \mathbf{x} ” has the same meaning as “jointly convex (resp., concave) in all dimensions of the vector \mathbf{x} ”.

⁴Note that the constraint of a convex (resp., concave) function being at most (resp., least) a constant is a convex constraint.

The concavity of $f_n(x)$ means decreasing marginal return, which often holds in various practical applications [17–20].

We also remark that $f_n(x)$, $f'_n(x)$ and $f''_n(x)$ are defined for any $x > 0$. Similar to the discussion in Footnote 1, for any of $f_n(x)$, $f'_n(x)$ and $f''_n(x)$, we do not require it to be defined for $x = 0$, but if it has a finite limit as $x \rightarrow 0^+$, we can just use the limit to define the corresponding value at $x = 0$. If there is no finite limit as $x \rightarrow 0^+$, then $f_n(x)$, $f'_n(x)$ or $f''_n(x)$ is not defined at $x = 0$.

For the specific expressions of the utility function $f_n(x)$, we will discuss three types in Section 4.4.

4.3 Challenges of solving Problem \mathbb{P}_1

Based on the proof of Lemma 4.4, we now call $\frac{f_n(r_{n,s}(p_n, B_n))}{p_n + p_n^{\text{cir}}}$ (i.e., $\varphi_n(p_n, B_n)$) a concave-convex ratio: a ratio having a concave function as the numerator and a convex function as the denominator. Then Problem \mathbb{P}_1 is maximizing the sum of concave-convex ratios. Such sum-of-ratios optimization is difficult to solve [21–23].

Lemma 4.4 also shows that $\varphi_n(p_n, B_n)$ for each n is pseudoconcave, unfortunately the sum of pseudoconcave functions may not be pseudoconcave. Even if we manage to prove the pseudoconcavity of $\sum_{n \in \mathcal{N}} c_n \varphi_n(p_n, B_n)$ (the objective function of \mathbb{P}_1), which is very difficult (e.g., just analyzing the pseudoconvexity of the sum of two linear fractional functions is already challenging as shown in [24]), then we can in principle use the KKT conditions of Problem \mathbb{P}_1 , as explained in⁵ Footnote 5, but those conditions involve taking derivatives of the ratios, inducing quite complex expressions, and the corresponding analysis becomes intractable. In this paper, instead of analyzing the pseudoconcavity of $\sum_{n \in \mathcal{N}} c_n \varphi_n(p_n, B_n)$ and being trapped in the intractable analysis, we will present an elegant approach (to be detailed in Section 5.1) for solving Problem \mathbb{P}_1 .

Recently, Shen and Yu [22, 23] proposed a novel technique to solve the sum-of-ratios optimization (referred to as fractional programming in their papers). However, since their technique relies on block coordinate ascent (i.e., alternating optimization), applying their technique to our Problem \mathbb{P}_1 will find a point which has no local or global optimality guarantee. In contrast, our approach will find a globally optimal solution of \mathbb{P}_1 .

4.4 Example utility functions for simulation

We provide three types of utility functions below since applications in the Metaverse will be diverse. In Section 7.1, we show that these functions well represent real data.

Type 1 utility function:

$$f_n(x) = \kappa_n \ln(1 + a_n x) \quad (7)$$

where $a_n, \kappa_n > 0$. This type is used in [17] as the reward function for sensing tasks.

Type 2 utility function:

$$f_n(x) = \kappa_n \cdot (1 - e^{-a_n x}) \quad (8)$$

where $a_n, \kappa_n > 0$, and e denotes the base of the natural logarithms. This type is motivated by [18] on mobile augmented reality.

Type 3 utility function:

$$f_n(x) = \kappa_n x^{a_n} \quad (9)$$

where $\kappa_n > 0$ and $0 < a_n < 1$. This function form has been used in prior work on congestion control [19] and mobile data subsidization [20]. In the terminologies of economics, the utility $\kappa_n r_{n,s}^{a_n}$ can be viewed as a Cobb–Douglas utility with respect to $r_{n,s}$, while the utility $\kappa_n \cdot (r_n - r_{n,e})^{a_n}$ can be regarded as a Stone–Geary utility with respect to r_n ; see Page 7 of [25].

It is straightforward to show that the above three types for the utility function all satisfy Condition 2 of Section 4.2. These three types are what we will use in the simulation of Section 7. We emphasize that our theoretical results (e.g., Algorithm 1 as well as Theorems 1 and 2 to be presented in Section 5) of this paper are applicable to **any** utility function satisfying Condition 2.

5 ALGORITHM TO FIND A GLOBAL OPTIMUM

In this section, we will discuss how to transform \mathbb{P}_1 into a sequence of convex optimization problems, and then use the transform to propose an algorithm that finds a global optimum of \mathbb{P}_1 .

5.1 Transforming Problem \mathbb{P}_1 into parametric convex optimization problems

Firstly, we introduce an auxiliary variable β_n to transform Problem \mathbb{P}_1 into the epigraph form. Let $\frac{c_n f_n(r_{n,s}(p_n, B_n))}{p_n + p_n^{\text{cir}}} \geq \beta_n$ and \mathbb{P}_1 can be transformed to the following equivalent form as \mathbb{P}_2 :

$$\text{Problem } \mathbb{P}_2: \max_{p, B, \beta} \sum_{n \in \mathcal{N}} \beta_n \quad (10)$$

$$\text{subject to: (4a), (4b),} \quad (10a)$$

$$F_n(p_n, B_n) - \beta_n \cdot (p_n + p_n^{\text{cir}}) \geq 0, \text{ for all } n \in \mathcal{N}, \quad (10b)$$

where we use $F_n(p_n, B_n)$ to simplify the representation:

$$F_n(p_n, B_n) := c_n f_n(r_{n,s}(p_n, B_n)). \quad (11)$$

Problem \mathbb{P}_2 is not convex optimization since $\beta_n \cdot (p_n + p_n^{\text{cir}})$ in (10b) is not jointly convex (actually also not jointly concave) in β_n and p_n , since the Hessian matrix for $\beta_n \cdot (p_n + p_n^{\text{cir}})$ is $\begin{bmatrix} 0 & 1 \\ 1 & 0 \end{bmatrix}$ which is not positive semidefinite (actually also not negative semidefinite).

We have explained in Section 4.3 that Problem \mathbb{P}_1 belongs to the following kind of problems: maximizing the sum of concave-convex ratios. Such kind of problems has a globally maximum according to [21, 22]. Hence, \mathbb{P}_1 and hence \mathbb{P}_2 have a global maximum.

To solve Problem \mathbb{P}_2 , one initial idea is trying to use Lemma 4.6 and hence the KKT conditions directly. Yet, deciding the quasi-convexity of $F_n(p_n, B_n) - \beta_n \cdot (p_n + p_n^{\text{cir}})$ in (10b) is very difficult. Hence, instead of trying to use \mathbb{P}_2 's KKT conditions directly, we take a step back and use the Fritz-John conditions (viz., Remark 4.2.2 of [14] and Lemma 2.1's proof in [21]), which do not need the quasiconvexity of constraints. The Fritz-John conditions provide the necessary conditions for a global optimum. Basically, in the Fritz-John conditions, the Lagrange multiplier (say w) on the gradient of the objective function can be zero or positive. Yet, following the proof of Lemma 2.1 in [21], we obtain $w > 0$. Then as shown in [21], w can be absorbed into other multipliers and hence omitted, after which the Fritz-John conditions reduce to the KKT conditions.

⁵For our maximization problem \mathbb{P}_1 , note that all constraints are clearly differentiable and convex (and hence quasiconvex) with Lemma 4.3 and Footnote 4. Hence, if we can prove that the objective function is pseudoconcave, then Lemma 4.6 means that we can use the KKT conditions to solve \mathbb{P}_1 . Nonetheless, even if we can do the above, the KKT conditions of \mathbb{P}_1 are intractable to obtain a solution.

Based on the above discussion, we have

any global maximum of \mathbb{P}_2 needs to satisfy the KKT conditions (14a)–(14l) below. (12)

For Problem \mathbb{P}_2 , with $\mathbf{v} := [\nu_n]_{n \in \mathcal{N}}$, $\boldsymbol{\tau} := [\tau_n]_{n \in \mathcal{N}}$ and λ denoting the multipliers, and the Lagrangian function given by

$$\begin{aligned} L_{\mathbb{P}_2}(\mathbf{p}, \mathbf{B}, \boldsymbol{\beta}, \mathbf{v}, \boldsymbol{\tau}, \lambda) \\ = -\sum_{n \in \mathcal{N}} \beta_n + \sum_{n \in \mathcal{N}} \nu_n \cdot (\beta_n \cdot (p_n + p_n^{\text{cir}}) - F_n(p_n, B_n)) \\ + \sum_{n \in \mathcal{N}} \tau_n \cdot (r_n^{\min} - r_n) + \lambda \cdot (\sum_{n \in \mathcal{N}} B_n - B_{\text{total}}), \end{aligned} \quad (13)$$

the KKT conditions of Problem \mathbb{P}_2 are as follows, with $L_{\mathbb{P}_2}$ short for $L_{\mathbb{P}_2}(\mathbf{p}, \mathbf{B}, \boldsymbol{\beta}, \mathbf{v}, \boldsymbol{\tau}, \lambda)$ (see [14, Theorem 4.2.3] or [16, Section 1.4.2] for a formal introduction of the KKT conditions):

Stationarity:

$$\frac{\partial L_{\mathbb{P}_2}}{\partial p_n} = 0, \text{ for all } n \in \mathcal{N}, \quad (14a)$$

$$\frac{\partial L_{\mathbb{P}_2}}{\partial B_n} = 0, \text{ for all } n \in \mathcal{N}, \quad (14b)$$

$$\frac{\partial L_{\mathbb{P}_2}}{\partial \beta_n} = -1 + \nu_n \cdot (p_n + p_n^{\text{cir}}) = 0, \text{ for all } n \in \mathcal{N}; \quad (14c)$$

Complementary slackness:

$$\nu_n \cdot (\beta_n \cdot (p_n + p_n^{\text{cir}}) - F_n(p_n, B_n)) = 0, \text{ for all } n \in \mathcal{N}, \quad (14d)$$

$$\tau_n \cdot (r_n^{\min} - r_n) = 0, \text{ for all } n \in \mathcal{N}, \quad (14e)$$

$$\lambda \cdot (\sum_{n \in \mathcal{N}} B_n - B_{\text{total}}) = 0; \quad (14f)$$

Primal feasibility:

$$F_n(p_n, B_n) - \beta_n \cdot (p_n + p_n^{\text{cir}}) \geq 0, \text{ for all } n \in \mathcal{N}, \quad (14g)$$

$$r_n(p_n, B_n) \geq r_n^{\min}, \text{ for all } n \in \mathcal{N}, \quad (14h)$$

$$\sum_{n \in \mathcal{N}} B_n \leq B_{\text{total}}; \quad (14i)$$

Dual feasibility:

$$\nu_n \geq 0, \text{ for all } n \in \mathcal{N}, \quad (14j)$$

$$\tau_n \geq 0, \text{ for all } n \in \mathcal{N}. \quad (14k)$$

$$\lambda \geq 0. \quad (14l)$$

From (14c), it follows that

$$\nu_n = \frac{1}{p_n + p_n^{\text{cir}}}, \quad (15)$$

and (14j) holds (actually the inequality sign in (14j) is taken).

Using (15) in (14d), we know

$$\beta_n = \frac{F_n(p_n, B_n)}{p_n + p_n^{\text{cir}}}, \quad (16)$$

and (14g) holds (actually the equal sign in (14g) is taken).

Instead of solving \mathbb{P}_2 's KKT conditions (14a)–(14l) directly, which is complex, we will connect them to a series of parametric convex optimization problems. In particular, supposing that $\boldsymbol{\beta}$ and \mathbf{v} are already given and satisfy (14c) (14d) (14g) and (14j), then we have the following result for the rest of \mathbb{P}_2 's KKT conditions:

$$(14a) (14b) (14e) (14f) (14h) (14i) (14k) \text{ and } (14l) \text{ together} \quad (17)$$

form the KKT conditions of Problem $\mathbb{P}_3(\boldsymbol{\beta}, \mathbf{v})$ below.

where we have

$$\begin{aligned} \text{Problem } \mathbb{P}_3(\boldsymbol{\beta}, \mathbf{v}): \quad & \max_{\mathbf{p}, \mathbf{B}} \sum_{n \in \mathcal{N}} \mathcal{F}_n(p_n, B_n | \beta_n, \nu_n) \\ \text{subject to: } & (4a), (4b). \end{aligned} \quad (18)$$

with $\mathcal{F}_n(p_n, B_n | \beta_n, \nu_n)$ defined as follows:

$$\mathcal{F}_n(p_n, B_n | \beta_n, \nu_n) := \nu_n \cdot (F_n(p_n, B_n) - \beta_n \cdot (p_n + p_n^{\text{cir}})). \quad (19)$$

Lemma 5.1 below states the relationship between \mathbb{P}_2 and \mathbb{P}_3 .

LEMMA 5.1. If $(\mathbf{p}^*, \mathbf{B}^*, \boldsymbol{\beta}^*)$ is a globally optimal solution of the Problem \mathbb{P}_2 , then $\boldsymbol{\beta}^*$ satisfies

$$\beta_n^* = \frac{F_n(p_n^*, B_n^*)}{p_n^* + p_n^{\text{cir}}}, \text{ for all } n \in \mathcal{N}. \quad (20)$$

Moreover, $(\mathbf{p}^*, \mathbf{B}^*)$ is a globally optimal solution to Problem $\mathbb{P}_3(\boldsymbol{\beta}^*, \mathbf{v}^*)$, with \mathbf{v}^* given by

$$\nu_n^* = \frac{1}{p_n^* + p_n^{\text{cir}}}, \text{ for all } n \in \mathcal{N}. \quad (21)$$

PROOF. Based on our analysis presented just before Lemma 5.1, we can easily prove Lemma 5.1 with the following:

- i) We establish (12) and (17) presented above.
- ii) Problem $\mathbb{P}_3(\boldsymbol{\beta}, \mathbf{v})$ belongs to convex optimization. In particular, the objective function to be maximized according to Lemma 4.4 and the definitions (11) (19), while the constraints are clearly convex with Lemma 4.3 (note that “concave \geq constant” is a convex constraint as noted in Footnote 5).
- iii) Slater's condition holds for Problem $\mathbb{P}_3(\boldsymbol{\beta}, \mathbf{v})$. In other words, there exists at least one point $[\mathbf{p}, \mathbf{B}]$ such that constraints (4a) and (4b) are satisfied with strict inequalities. An example is as follows: with B_n being $\frac{B_{\text{total}}}{2N}$ for all $n \in \mathcal{N}$, set p_n such that $r_n(p_n, B_n) = 2r_n^{\min}$ for all $n \in \mathcal{N}$.
- iv) Results “ii)” and “iii)” above together with Lemma 4.5 mean that given $(\boldsymbol{\beta}, \mathbf{v})$, then (\mathbf{p}, \mathbf{B}) is a globally optimal solution to Problem $\mathbb{P}_3(\boldsymbol{\beta}, \mathbf{v})$ if and only if $\mathbb{P}_3(\boldsymbol{\beta}, \mathbf{v})$'s KKT conditions (14a) (14b) (14e) (14f) (14h) (14i) (14k) and (14l) are satisfied.
- v) (20) and (21) specifying $(\boldsymbol{\beta}^*, \mathbf{v}^*)$ follow from (15) and (16).

In addition to the above explanation, interested readers can also refer to Lemma 2.1 and Remark 2.1 of [21], where Lemma 2.1 of [21] handles minimizing the sum of convex-concave ratios and Remark 2.1 of [21] addresses maximizing the sum of concave-convex ratios (i.e., the case of our Problem \mathbb{P}_1). \square

With Lemma 5.1 presented above, we now describe how to solve Problem \mathbb{P}_2 using $\mathbb{P}_3(\boldsymbol{\beta}, \mathbf{v})$. Let $[\mathbf{p}^\#(\boldsymbol{\beta}, \mathbf{v}), \mathbf{B}^\#(\boldsymbol{\beta}, \mathbf{v})]$ denote a globally optimal solution to $\mathbb{P}_3(\boldsymbol{\beta}, \mathbf{v})$, where $\mathbf{p}^\#(\boldsymbol{\beta}, \mathbf{v}) = [p_n^\#(\boldsymbol{\beta}, \mathbf{v})]_{n \in \mathcal{N}}$ and $\mathbf{B}^\#(\boldsymbol{\beta}, \mathbf{v}) = [B_n^\#(\boldsymbol{\beta}, \mathbf{v})]_{n \in \mathcal{N}}$. We further define

$$\phi_{1,n}(\boldsymbol{\beta}, \mathbf{v}) := -F_n(p_n^\#(\boldsymbol{\beta}, \mathbf{v}), B_n^\#(\boldsymbol{\beta}, \mathbf{v})) + \beta_n \cdot (p_n^\#(\boldsymbol{\beta}, \mathbf{v}) + p_n^{\text{cir}}), \quad (22)$$

$$\phi_{2,n}(\boldsymbol{\beta}, \mathbf{v}) := -1 + \nu_n \cdot (p_n^\#(\boldsymbol{\beta}, \mathbf{v}) + p_n^{\text{cir}}), \quad (23)$$

$$\phi_1(\boldsymbol{\beta}, \mathbf{v}) := [\phi_{1,n}(\boldsymbol{\beta}, \mathbf{v})]_{n \in \mathcal{N}}, \quad \phi_2(\boldsymbol{\beta}, \mathbf{v}) := [\phi_{2,n}(\boldsymbol{\beta}, \mathbf{v})]_{n \in \mathcal{N}},$$

$$\boldsymbol{\phi}(\boldsymbol{\beta}, \mathbf{v}) := [\phi_1(\boldsymbol{\beta}, \mathbf{v}), \phi_2(\boldsymbol{\beta}, \mathbf{v})]. \quad (24)$$

With $(\mathbf{p}^*, \mathbf{B}^*, \boldsymbol{\beta}^*)$ denoting a globally optimal solution of Problem \mathbb{P}_2 (and hence $(\mathbf{p}^*, \mathbf{B}^*)$ denoting a globally optimal solution of Problem \mathbb{P}_1), clearly setting $(\boldsymbol{\beta}, \mathbf{v})$ as $(\boldsymbol{\beta}^*, \mathbf{v}^*)$ of (20) and (21) satisfies

$$\boldsymbol{\phi}(\boldsymbol{\beta}, \mathbf{v}) = \mathbf{0}. \quad (25)$$

Based on the above, solving Problem \mathbb{P}_2 and hence \mathbb{P}_1 can be transformed into solving (25) to obtain $\mathbb{P}_3(\boldsymbol{\beta}^*, \mathbf{v}^*)$, and then set $[\mathbf{p}^*, \mathbf{B}^*]$ as $[\mathbf{p}^\#(\boldsymbol{\beta}^*, \mathbf{v}^*), \mathbf{B}^\#(\boldsymbol{\beta}^*, \mathbf{v}^*)]$, a globally optimal solution to $\mathbb{P}_3(\boldsymbol{\beta}^*, \mathbf{v}^*)$, according to Lemma 5.1. Based on the above idea, we present Algorithm 1 next, where it will become clear that solving \mathbb{P}_1 becomes solving a series of parametric convex optimization $\mathbb{P}_3(\boldsymbol{\beta}^{(i)}, \mathbf{v}^{(i)})$, with i denoting the iteration index. (26)

5.2 Our Algorithm 1 to solve Problem \mathbb{P}_1

As explained in the previous subsection, we solve (25) first in order to obtain a globally optimal solution to Problem \mathbb{P}_1 . Root-finding algorithms such as Newton's method can be used to solve (25). Our

Algorithm 1 actually uses a modified Newton method of [21], which always converges to the desired solution. In contrast, the original Newton's method is sensitive to initialization (e.g., no convergence if starting at bad initialization, as shown in Section 4 of [21]).

Algorithm 1 starts with computing the initial $[\beta^{(0)}, \mathbf{v}^{(0)}]$ from $[\mathbf{p}^{(0)}, \mathbf{B}^{(0)}]$, as shown in the pseudocode. In the i -th iteration of Algorithm 1 (i starts from 0), we update $[\beta^{(i)}, \mathbf{v}^{(i)}]$ to $[\beta^{(i+1)}, \mathbf{v}^{(i+1)}]$ based on (28) (29) (30) (31), which essentially present the modified Newton method to solve (25). The numerators in (29) (30) use $(\partial\phi_{1,n}(\beta^{(i)}, \mathbf{v}^{(i)}))/(\partial\beta_n)$ and $(\partial\phi_{2,n}(\beta^{(i)}, \mathbf{v}^{(i)}))/(\partial v_n)$, which are shown in our full version [26] to be equal to

$$p_n^\#(\beta^{(i)}, \mathbf{v}^{(i)}) + p_n^{\text{cir}}. \quad (27)$$

The denominators in (29) (30) use $\phi_{1,n}(\beta^{(i)}, \mathbf{v}^{(i)})$ and $\phi_{2,n}(\beta^{(i)}, \mathbf{v}^{(i)})$, whose computations based on (22) (23) require obtaining $[\mathbf{p}^\#(\beta^{(i)}, \mathbf{v}^{(i)}), \mathbf{B}^\#(\beta^{(i)}, \mathbf{v}^{(i)})]$ by solving Problem $\mathbb{P}_3(\beta^{(i)}, \mathbf{v}^{(i)})$. This is the reason why we have (26).

We remark that in Algorithm 1, the iterative process of computing $[\mathbf{p}^\#(\beta^{(i)}, \mathbf{v}^{(i)}), \mathbf{B}^\#(\beta^{(i)}, \mathbf{v}^{(i)})]$ and then using it for updating $[\beta^{(i)}, \mathbf{v}^{(i)}]$ to $[\beta^{(i+1)}, \mathbf{v}^{(i+1)}]$ is not the classical dual gradient descent (DGD) [27] despite the resemblance, since β is not a Lagrange multiplier. Algorithm 1 solves (25) using the modified Newton method, while DGD involves maximizing the dual function.

We formally state the solution quality of Algorithm 1 as follows.

THEOREM 1. *Under Conditions 1 and 2 of Section 4, our proposed Algorithm 1 finds a **globally optimal** solution to Problem \mathbb{P}_1 (up to arbitrary accuracy).*

PROOF. The analyses above in Sections 5.1 and 5.2, stated before Theorem 1, have already provided the proof of Theorem 1. \square

Next, we discuss the fast convergence and order-optimal time complexity of Algorithm 1. As shown in Theorem 3.2 of [21], the modified Newton method used in Algorithm 1 has global linear and local quadratic rates of convergence.

To analyze the time complexity, we use floating point operations (flops). One addition/subtraction/multiplication/division is one flop. We now analyze Lines 3–8, the main part of Algorithm 1. Suppose that in Line 4, we use the bisection method to obtain $\lambda^\#$ from (34), for which there are K iterations and each iteration has $O(N)$, where K depends on the error tolerance, as detailed in our full version [26]. Hence, Line 4 consumes $O(LN)$. Lines 5, 6, and 8 cost $O(N)$ flops. Line 7 takes $O((J_i + 2)N)$ flops. Suppose the loop in Line 3 needs \mathcal{I} iterations before convergence (\mathcal{I} is less than 10 in our experiments to find a 0.01-global optimum, which means the relative difference between the objective-function values under the found solution and the true global optimum is at most 0.01). Then the time complexity of Algorithm 1 is $O(IKN + \sum_{i=0}^{\mathcal{I}-1} (J_i + 2)N)$, which is linear in N . This linear complexity is the best that any algorithm can do, since we need to decide N number of $[B_n, p_n]$ for all N users. Hence, Algorithm 1 achieves the optimal time complexity in the order sense.

5.3 Solving Problem $\mathbb{P}_3(\beta, \mathbf{v})$

From (26), solving Problem \mathbb{P}_1 requires solving a series of $\mathbb{P}_3(\beta, \mathbf{v})$. One approach is to use the CVX tool [16]. However, the worst-case complexity of global convex optimization grows exponentially with

Algorithm 1: Our approach to compute a **globally optimal** solution $[\mathbf{p}, \mathbf{B}]$ (up to arbitrary accuracy) to Problem \mathbb{P}_1 of Section 3.2 on utility-energy efficiency optimization.

- 1 Initialize feasible $[\mathbf{p}^{(0)}, \mathbf{B}^{(0)}]$, $i = 0$, $\xi \in (0, 1)$, $\epsilon \in (0, 1)$.
- 2 Calculate $\beta^{(0)} = [\beta_n^{(0)}]_{n \in \mathcal{N}}$ and $\mathbf{v}^{(0)} = [v_n^{(0)}]_{n \in \mathcal{N}}$ via

$$\beta_n^{(0)} = \frac{c_n f_n(r_{n,s}(p_n^{(0)}, B_n^{(0)}))}{p_n^{(0)} + p_n^{\text{cir}}}, \quad v_n^{(0)} = \frac{1}{p_n^{(0)} + p_n^{\text{cir}}}.$$

3 **repeat**

- 4 Use Eq. (32) in Theorem 2 on Page 8 to solve $\mathbb{P}_3(\beta^{(i)}, \mathbf{v}^{(i)})$, and obtain a solution $[\mathbf{p}^\#(\beta^{(i)}, \mathbf{v}^{(i)}), \mathbf{B}^\#(\beta^{(i)}, \mathbf{v}^{(i)})]$.
- 5 Use $[\mathbf{p}^\#(\beta^{(i)}, \mathbf{v}^{(i)}), \mathbf{B}^\#(\beta^{(i)}, \mathbf{v}^{(i)})]$ obtained above to compute $\phi(\beta^{(i)}, \mathbf{v}^{(i)})$ according to Eq. (24) on Page 6.
- 6 If $\phi(\beta^{(i)}, \mathbf{v}^{(i)})$ is the zero vector, then $[\mathbf{p}^\#(\beta^{(i)}, \mathbf{v}^{(i)}), \mathbf{B}^\#(\beta^{(i)}, \mathbf{v}^{(i)})]$ is the global optimal solution to Problem \mathbb{P}_1 and we finish the algorithm.
- 7 Otherwise, let J_i be the smallest integer that satisfies

$$\begin{aligned} & \|\phi(\beta^{(i)} + \xi^{J_i} \sigma_1^{(i)}, \mathbf{v}^{(i)} + \xi^{J_i} \sigma_2^{(i)})\|_2 \\ & \leq (1 - \xi^{J_i} \epsilon) \cdot \|\phi(\beta^{(i)}, \mathbf{v}^{(i)})\|_2, \end{aligned} \quad (28)$$

where “ $\|\cdot\|_2$ ” denotes the Euclidean norm, the n th-dimension of $\sigma_1^{(i)}$ (resp. $\sigma_2^{(i)}$) for $n \in \mathcal{N}$, denoted by $\sigma_1^{(i)}[n]$ (resp. $\sigma_2^{(i)}[n]$), is given by

$$\sigma_1^{(i)}[n] := -\frac{(\partial\phi_{1,n}(\beta^{(i)}, \mathbf{v}^{(i)}))/(\partial\beta_n)}{\phi_{1,n}(\beta^{(i)}, \mathbf{v}^{(i)})} \quad (29)$$

$$= -\frac{(27)}{\text{RHS of (22) with } (\beta, \mathbf{v}) \text{ being } (\beta^{(i)}, \mathbf{v}^{(i)})},$$

$$\sigma_2^{(i)}[n] := -\frac{(\partial\phi_{2,n}(\beta^{(i)}, \mathbf{v}^{(i)}))/(\partial v_n)}{\phi_{2,n}(\beta^{(i)}, \mathbf{v}^{(i)})} \quad (30)$$

$$= -\frac{(27)}{\text{RHS of (23) with } (\beta, \mathbf{v}) \text{ being } (\beta^{(i)}, \mathbf{v}^{(i)})},$$

where RHS is short for the right hand side.

//Comment: Obtaining J_i above involves evaluating $(J_i + 2)$ number of $\phi(\beta, \mathbf{v})$ for (28). To compute each of them, we need to solve Problem $\mathbb{P}_3(\beta, \mathbf{v})$ via (32) on Page 8 to obtain $[\mathbf{p}^\#(\beta, \mathbf{v}), \mathbf{B}^\#(\beta, \mathbf{v})]$, and then apply (24) on Page 6.

8 **Update**

$$(\beta^{(i+1)}, \mathbf{v}^{(i+1)}) \leftarrow (\beta^{(i)} + \xi^{J_i} \sigma_1^{(i)}, \mathbf{v}^{(i)} + \xi^{J_i} \sigma_2^{(i)}), \quad (31)$$

where J_i is obtained from (28).

//Comment: If J_i happens to be 0, then (31) becomes the standard Newton method as explained in the last paragraph on Page 13 of [21]. As shown by Problem 2 on Page 14 of [21], the standard Newton method may fail for some initial points, so we follow [21] to find J_i according to (28) instead of always setting J_i as 0.

9 **Let** $i \leftarrow i + 1$.

10 **until** $\phi(\beta^{(i)}, \mathbf{v}^{(i)})$ is close to 0;

- 11 Use the current $[\beta, \mathbf{v}]$ in (32) on Page 8 and return the obtained $[\mathbf{p}^\#(\beta, \mathbf{v}), \mathbf{B}^\#(\beta, \mathbf{v})]$ as the solution to Problem \mathbb{P}_1 .
-

the problem size N from Section 1.4.2 of [16]. Based on Theorem 2 below, we can solve $\mathbb{P}_3(\beta, \nu)$ and hence \mathbb{P}_1 in linear time with respect to N , as discussed in the previous subsection.

THEOREM 2. *Under Conditions 1 and 2 of Section 4, any **globally optimal** solution $[P^\#(\beta, \nu), B^\#(\beta, \nu)]$ to Problem $\mathbb{P}_3(\beta, \nu)$ defined in (18) can be given as follows:*

$$\begin{cases} B_n^\#(\beta, \nu) = \mathcal{B}_n(\lambda^\#) \text{ for all } n \in \mathcal{N}, \\ P_n^\#(\beta, \nu) = \frac{\sigma_n^2 B_n^\#(\beta, \nu) \cdot \psi_n(\lambda^\#)}{g_n} \text{ for all } n \in \mathcal{N}, \end{cases} \quad (32)$$

with function $\mathcal{B}_n(\lambda)$ defined by

$$\mathcal{B}_n(\lambda) := \frac{\max\{\gamma_n(\lambda), r_n^{\min}\}}{\log_2(1 + \psi_n(\lambda))}, \quad (33)$$

and $\lambda^\#$ denoting the solution to

$$\sum_{n \in \mathcal{N}} \mathcal{B}_n(\lambda) = B_{\text{total}} \quad (34)$$

where $\psi_n(\lambda)$ and $\gamma_n(\lambda)$ are defined by

$$\psi_n(\lambda) := \exp\left\{1 + W\left(\frac{1}{e} \left(\frac{g_n \lambda}{\nu_n \beta_n \sigma_n^2} - 1\right)\right)\right\} - 1, \quad (35)$$

for $W(\cdot)$ being the principal branch of the Lambert W function

($W(z)$ for $z \geq -e^{-1}$ is the solution of $x \geq -1$ to the equation $xe^x = z$),

$$\text{and } \gamma_n(\lambda) - r_{n,e} := \begin{cases} \xi := (f'_n)^{-1}\left(\frac{\beta_n \sigma_n^2 (1 + \psi_n(\lambda)) \ln 2}{c_n g_n}\right) \\ \text{when such result } \xi \geq 0 \text{ exists,} \\ 0, \text{ otherwise,} \end{cases} \quad (36)$$

with $(f'_n)^{-1}(\cdot)$ denoting the inverse function of the derivative $f'_n(\cdot)$.

Theorem 2 is proved in our full version [26], where we also elaborate the bisection method to obtain $\lambda^\#$ from (34).

6 INSIGHTS FROM OUR OPTIMIZATION

In this section, we review our optimization technique used in Algorithm 1 to obtain the insights, which can be used to solve many other problems in wireless networks and mobile computing.

In Section 5.1, Problem \mathbb{P}_2 is not convex optimization since we have the non-convex product term $\beta_n \cdot (p_n + p_n^{\text{cir}})$ in (10b), as shown in the sentences following (11). The solving process of \mathbb{P}_2 is transformed into solving a series of parametric convex optimization $\mathbb{P}_3(\beta, \nu)$ where $[\beta, \nu]$ is given so that there is no non-convex product term and we have convex optimization. The solving of each \mathbb{P}_3 is used to update $[\beta, \nu]$ under which \mathbb{P}_3 is solved again with the new $[\beta, \nu]$, where the update of $[\beta, \nu]$ is based on the KKT conditions of \mathbb{P}_2 .

From the above discussion, we can identify the following:

Our technique to handle functions of product or quotient terms in optimization: With “ \ast ” denoting multiplication or division, if there are terms $f_n(A_n(x) \ast y_n) |_{n \in \mathcal{N}}$ in an optimization problem \mathbb{P} , for functions $f_n, A_n |_{n \in \mathcal{N}}$ and variables x and $y = [y_n |_{n \in \mathcal{N}}]$, we can convert \mathbb{P} into a series of parametric convex optimization $\mathbb{Q}(y, z)$, where z comprise additional variables in the parameterization (e.g., ν in our “ $\mathbb{P}_3(\beta, \nu)$ ”). In $\mathbb{Q}(y, z)$, given $[y, z]$, variables in $A_n(x) \ast y_n$ just have x , so that \mathbb{Q} can be easier to solve than \mathbb{P} , or \mathbb{Q} may even happen to be convex in x . The solving of each \mathbb{Q} will be used to update $[y, z]$ under which \mathbb{Q} is solved again with the new $[y, z]$, where the update of $[y, z]$ is based on the KKT conditions of \mathbb{P} .

With the above technique, we can also address $f_n(A_n(x) \ast B_n(x)) |_{n \in \mathcal{N}}$ in optimization, for functions $f_n, A_n, B_n |_{n \in \mathcal{N}}$ and variables x . We replace $A_n(x) \ast B_n(x)$ by an auxiliary variable z_n and

enforce the constraint of z_n being either no greater or no less than $A_n(x) \ast B_n(x)$ (depending on the specific problem), where the constraint can be further converted into a relationship between $A_n(x)$ and $z_n \ast B_n(x)$, like how we transform \mathbb{P}_1 of (4) to \mathbb{P}_2 of (10).

To summarize, our technique can be useful for various optimization problems involving product or quotient terms. In addition, the technique often obtains a global optimum, as in Theorem 1. The above finding goes beyond the sum-of-ratios optimization of [21], although our original motivation comes from [21]. The following discussion shows that our above finding is very likely to be new.

Two recent papers [22, 23] by Shen and Yu have been considered breakthroughs in fractional programming, as seen from their high citations (684 and 188 respectively as of 7 March 2023 in Google Scholar). However, they find neither local nor global optimum. In contrast, our technique above will find a global optimum. Interested readers can refer to our full version [26].

Our above technique can be applied to many optimization problems in wireless networks and mobile computing, as illustrated by two examples below. In interference-constrained wireless networks, globally solving the weighted sum-rate maximization (WSRM) efficiently was an open problem for years before it was addressed by [28], since a user’s rate (per unit bandwidth) given by $\log_2(1 + \frac{\text{TransmitPower}}{\text{Interference+Noise}})$ involves a fraction inside a logarithm, which is difficult to deal with. Our technique above will find a global optimum for WSRM and other problems involving the above rate expression, while the polyblock-based approach of [28] relies on the structure of WSRM and may not be applied to other problems. In mobile edge computing, with γ denoting the offloading ratio of computation tasks, [29] minimizes the system cost, given by $\gamma \cdot \text{EdgeComputingCost} + (1 - \gamma) \cdot \text{LocalComputingCost}$. The multiplication above means no joint convexity in γ and other variables. Then [29] uses alternating optimization which is neither locally nor globally optimal, while our technique will find a global optimum.

7 SIMULATION

In Section 7.1, we use real data to model the utility functions. Then we will conduct simulations to illustrate the effectiveness of our Algorithm 1. Specifically, we present the parameter settings in Section 7.2, before reporting simulation results in other subsections.

7.1 Modeling the utility from real data

The primary concern in the quality of experience (QoE) design is creating a human-perceived utility function. To accurately measure a user’s subjective perception of video quality, we utilize the SSV dataset [30], which is constructed by real VR users in 360° video scenarios. Besides, we also leverage the VMAF dataset in Netflix Public Dataset⁶ to obtain more comprehensive subjective scores of videos. Our utility functions, e.g., three types of utility functions introduced in Section 4.4, are constructed based on these inclusive datasets, which cover a wide range of factors including resolution, bit rate, and experience scores of the VR users and videos. Note that, the scores in the SSV dataset are based on the mean opinion score (MOS) ranging from 1 to 5, and the scores in the VMAF dataset are the differential mean opinion score (DMOS) ranging from 1 to 100.

⁶<https://github.com/Netflix/vmaf/blob/master/resource/doc/datasets.md>

In Fig. 2 (a), we present three curves of utility functions from the SSV dataset, which correspond to the three scenarios of user 1 sitting, user 2 sitting, and user 1 standing with the resolution of 2K and watching the same video. Another three curves of utility functions from the VMAF dataset are shown in Fig. 2 (b) with three different videos. In Table 1, we give the detailed expression of those utility functions.

Table 1: The detailed expression of utility functions in Fig. 2, where x denotes the bit rate in M bps and y denotes the resolution in M pixels.

utility function	scenario	dataset
$f_1(x) = 0.5424 \ln(1 + 37.2965x)$	user 1 seated	SSV
$f_2(x) = 2.9351(1 - e^{-2.1224x})$	user 2 seated	SSV
$f_3(x) = 3.2956(x/15.94)^{0.2733}$	user 1 standing	SSV
$f_4(x) = 103.3464(1 - e^{-2.9792y - 0.23166x})$	video 1	VMAF
$f_5(x) = 33.4215 \ln(1 + 10.0826y + 0.784x)$	video 2	VMAF
$f_6(x) = 61.8622(x/15 + y/1.1664)^{0.5301}$	video 3	VMAF

7.2 Parameter setting

We first state settings that apply to all simulations. Based on [31], we model the pass loss between each legitimate user and the Metaverse server as $128.1 + 37.6 \log(\text{distance})$ along with 8 decibels (dB) as the standard deviation of shadow fading, and the unit of *distance* is kilometer. The power spectral density of Gaussian noise σ_n^2 is -174 dBm/Hz (i.e., 4 zeptowatts/Hz, the value for thermal noise at 20 °C room temperature [32]).

In addition, some default settings are as follows, unless otherwise specified. N denoting the number of legitimate users is 30. The weight parameter c_n is set to 1 for all users (unless configured otherwise), which means the weighted sum-UEE just becomes sum-UEE. The default total bandwidth B_{total} is 20 MHz. The circuit power p_n^{cir} is 2 dBm (i.e., 1.6 milliwatts) for each n . Both the eavesdropping rate $r_{n,e}$ and the minimum transmission rate r_n^{\min} are 20 kilobits per second (Kbps) by default. For all types of utility functions, κ_n is 1 and a_n is 0.5 by default. In all cases, we stop the algorithm after obtaining a 0.01-global optimum, whose meaning has been discussed in Section 5.2.

7.3 Comparison of different algorithms

We now compare the proposed Algorithm 1 with the following baseline algorithms:

- (i) **Optimize B only:** Here we let p_n for each n be 1 mW (i.e., 10^{-3} W), which will be substituted into Problem \mathbb{P}_1 . Then “optimizing B only” becomes convex optimization, for which the KKT conditions are analyzed to obtain the solution.
- (ii) **Optimize p only:** In this case, we let B_n for each n be B_{total}/N , which will be substituted into Problem \mathbb{P}_1 . Then “optimizing p only” becomes convex optimization, for which the KKT conditions are analyzed to obtain the solution.
- (iii) **Alternating optimization:** starting with a feasible initialization, we perform “(i)” and “(ii)” above in an alternating manner,

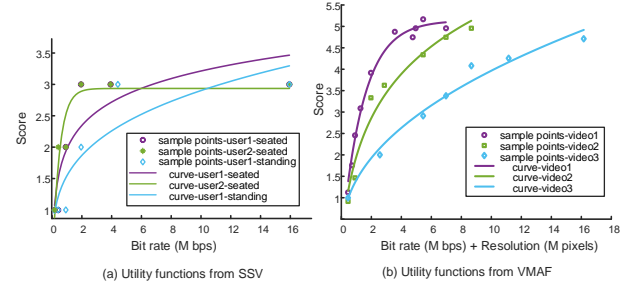


Figure 2: The fitting results of utility functions under different scenarios.

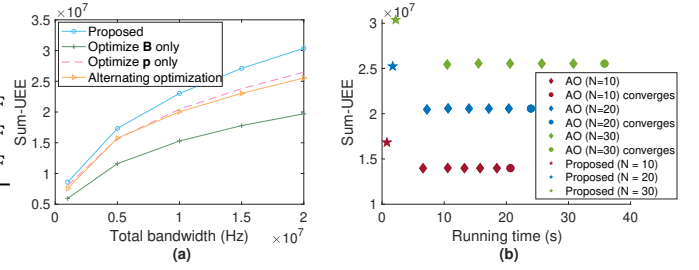


Figure 3: (a). Algorithms with respect to the total bandwidth. (b). Running time and objective-function value under each algorithm, where AO is short for alternating optimization.

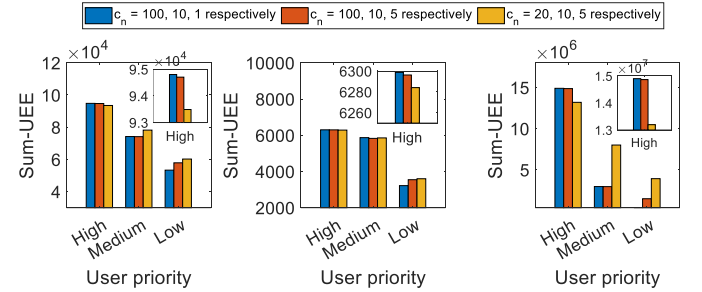


Figure 4: Sum-UEE for high-, medium-, and low-priority users, under different c_n combinations, where subfigures (a) (b) and (c) are for utility functions of Types 1, 2, and 3, respectively.

until convergence (when the relative increase between two consecutive iterations is negligible).

For the detailed analyses of the baseline algorithms, interested readers can refer to our full version [26].

We compare Algorithm 1 with the above algorithms in Fig. 3, where Type 3 utility function is used. Fig. 3(a) plots the sum-UEE with respect to the total bandwidth B_{total} . The curves show that our proposed algorithm achieves larger sum-UEE than all the baseline algorithms. It can be observed that as B_{total} increases, UEE grows but at a progressively slower rate. This is intuitive to understand since each user’s UEE is an increasing and concave function with respect to the bandwidth, given the transmission power.

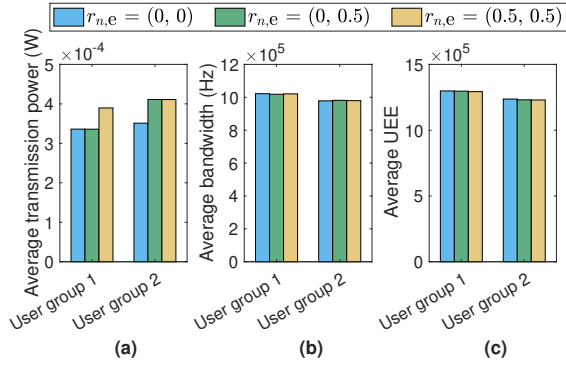


Figure 5: Setting different $r_{n,e}$ for two user groups, where the legend $r_{n,e} = (a, b)$ means that $r_{n,e}$ for user U_n in Group 1 is set as $a \cdot r_n^{\min}$ while $r_{n,e}$ for user U_n in Group 2 is set as $b \cdot r_n^{\min}$.

In Fig. 3(b), the convergence performance of our proposed algorithm and alternating optimization (AO) is displayed. We evaluate the two algorithms under different N , respectively. It is obvious that our proposed algorithm always obtains a better sum-UEE and converges much faster. In particular, on a laptop with 8GB of RAM and 256GB of storage, the proposed algorithm converges within 3 seconds, but AO algorithm takes around 35, 25, 20 seconds under $N = 10, 20, 30$, respectively.

7.4 The priority level of users

Then we explore the influence of the priority of users under different utility functions. Assume that users are evenly classified into three different priority levels, corresponding to different weights c_n . The larger the c_n , the higher the priority level, the more resource would be allocated and thus the greater the UEE.

Fig. 4 shows UEE of users with different priority levels based on three types of different functions. We first compare results from $c_n = 100, 10, 1$ and $c_n = 100, 10, 5$, $c_n = 20, 10, 1$ and $c_n = 20, 10, 5$. The results show an increase in efficiency of low priority users and a slight decrease of other 2 groups, as expected. This is because as c_n grows from 1 to 5, proposed algorithm would allocate more bandwidth resource from high and medium users to low priority users (Recall that efficiency is increasing with respect to B_n). Accordingly, if we reduce c_n from $c_n = 100, 10, 1$ and $c_n = 100, 10, 5$ to $c_n = 20, 10, 1$ and $c_n = 20, 10, 5$ respectively, a decrease could be observed in efficiency of users with high priority. Conversely, that of users with medium and low priority will see growth. Therefore, the above results demonstrate the validity of the priority level weighting factor c_n .

7.5 Impact of individual rate constraints

In the final, we analyze the effect of changing $r_{n,e}$ on the experimental results in Fig. 5. The number of users N is set as 20 and we divided them equally into two groups with different $r_{n,e}$ for comparison. From Fig. 5(a), we can see when both groups have the same change in $r_{n,e}$, e.g., from $(0, 0)$ to $(0.5, 0.5)$, the difference in average transmission power between them does not change obviously. Only when $r_{n,e}$ of one group is greater than that of the other,

does the average transmission power of former increase accordingly. Average bandwidth in Fig. 5(b) also has the same trend as the average transmission power, but relatively smaller. The average UEE decreases as $r_{n,e}$ grows, which seems intuitive since the utility is $f_n(r_n(p_n, B_n) - r_{n,e})$.

For more simulation results (e.g., how our proposed algorithm performs when the number of users changes or when there are heterogeneous types of utility functions among the users), interested readers can refer to our full version [26].

8 CONCLUSION

In our paper, we have proposed Metaverse utility-energy efficiency (UEE) that considers physical layer security to measure the efficient degree of energy consumption. Diverse utility functions can be applied to meet the requirements of different Metaverse scenarios. We propose an algorithm with order-optimal time complexity to maximize the overall weighted UEE of a Metaverse system by optimizing transmission power and bandwidth allocation. A globally optimal solution can be found and simulations demonstrate the effectiveness of our algorithm, which has better convergence performance and faster speed compared to baseline approaches.

REFERENCES

- [1] Y. Wang, Z. Su, N. Zhang, R. Xing, D. Liu, T. H. Luan, and X. Shen, "A survey on Metaverse: Fundamentals, security, and privacy," *IEEE Communications Surveys & Tutorials*, 2022.
- [2] J.-M. Chung, "XR HMDs and detection technology," in *Emerging Metaverse XR and Video Multimedia Technologies: Modern Streaming and Multimedia Systems and Applications*, 2022, pp. 99–139.
- [3] V. Nair, G. M. Garrido, and D. Song, "Exploring the unprecedented privacy risks of the Metaverse," *arXiv preprint arXiv:2207.13176*, 2022.
- [4] X. Huang, W. Xu, H. Shen, H. Zhang, and X. You, "Utility-energy efficiency oriented user association with power control in heterogeneous networks," *IEEE Wireless Communications Letters*, vol. 7, no. 4, pp. 526–529, 2018.
- [5] D. Wang, B. Bai, W. Chen, and Z. Han, "Achieving high energy efficiency and physical-layer security in af relaying," *IEEE Transactions on Wireless Communications*, vol. 15, no. 1, pp. 740–752, 2015.
- [6] T. Wang and L. Vandendorpe, "On the optimum energy efficiency for flat-fading channels with rate-dependent circuit power," *IEEE transactions on communications*, vol. 61, no. 12, pp. 4910–4921, 2013.
- [7] F. Guo, F. R. Yu, H. Zhang, H. Ji, V. C. Leung, and X. Li, "An adaptive wireless virtual reality framework in future wireless networks: A distributed learning approach," *IEEE Transactions on Vehicular Technology*, vol. 69, no. 8, pp. 8514–8528, 2020.
- [8] A. D. Wyner, "The wire-tap channel," *Bell System Technical Journal*, vol. 54, no. 8, pp. 1355–1387, 1975.
- [9] I. Csiszár and J. Körner, "Broadcast channels with confidential messages," *IEEE Transactions on Information Theory*, vol. 24, no. 3, pp. 339–348, 1978.
- [10] A. Yener and S. Ulukus, "Wireless physical-layer security: Lessons learned from information theory," *Proceedings of the IEEE*, vol. 103, no. 10, pp. 1814–1825, 2015.
- [11] J. Barros and M. R. Rodrigues, "Secrecy capacity of wireless channels," in *IEEE International Symposium on Information Theory*, 2006, pp. 356–360.
- [12] J. Xu and R. Zhang, "Throughput optimal policies for energy harvesting wireless transmitters with non-ideal circuit power," *IEEE Journal on Selected Areas in Communications*, vol. 32, no. 2, pp. 322–332, 2013.
- [13] Y. Jiang, Y. Zou, J. Ouyang, and J. Zhu, "Secrecy energy efficiency optimization for artificial noise aided physical-layer security in OFDM-based cognitive radio networks," *IEEE Transactions on Vehicular Technology*, vol. 67, no. 12, pp. 11 858–11 872, 2018.
- [14] A. Cambini and L. Martein, *Generalized convexity and optimization: Theory and applications*. Springer Science & Business Media, 2008, vol. 616.
- [15] X. Zhou, J. Zhao, H. Han, and C. Guet, "Joint optimization of energy consumption and completion time in federated learning," in *2022 IEEE 42nd International Conference on Distributed Computing Systems (ICDCS)*, 2022, pp. 1005–1017.
- [16] S. Boyd and L. Vandenberghe, *Convex Optimization*. Cambridge University Press, 2004.
- [17] D. Yang, G. Xue, X. Fang, and J. Tang, "Crowdsourcing to smartphones: Incentive mechanism design for mobile phone sensing," in *Proceedings of the 18th annual international conference on Mobile computing and networking*, 2012, pp. 173–184.

- [18] Q. Liu, S. Huang, J. Opadere, and T. Han, "An edge network orchestrator for mobile augmented reality," in *IEEE INFOCOM 2018-IEEE Conference on Computer Communications*. IEEE, 2018, pp. 756–764.
- [19] J. Mo and J. Walrand, "Fair end-to-end window-based congestion control," *IEEE/ACM Transactions on Networking*, vol. 8, no. 5, pp. 556–567, 2000.
- [20] Z. Xiong, J. Zhao, D. Niyato, R. Deng, and J. Zhang, "Reward optimization for content providers with mobile data subsidization: A hierarchical game approach," *IEEE Transactions on Network Science and Engineering*, vol. 7, no. 4, pp. 2363–2377, 2020.
- [21] Y. Jong, "An efficient global optimization algorithm for nonlinear sum-of-ratios problem," *Optimization Online*, pp. 1–21, 2012.
- [22] K. Shen and W. Yu, "Fractional programming for communication systems-Part I: Power control and beamforming," *IEEE Transactions on Signal Processing*, vol. 66, no. 10, pp. 2616–2630, 2018.
- [23] —, "Fractional programming for communication systems-Part II: Uplink scheduling via matching," *IEEE Transactions on Signal Processing*, vol. 66, no. 10, pp. 2631–2644, 2018.
- [24] A. Cambini, L. Martein, and S. Schaible, "On the pseudoconvexity of the sum of two linear fractional functions," in *7th International Symposium on Generalized Convexity and Generalized Monotonicity*, 2005, pp. 161–172.
- [25] W. da Cruz Vieira, A. Bucci, and S. Marsiglio, "Welfare and convergence speed in the Ramsey model under two classes of Gorman preferences," *Italian Economic Journal*, vol. 7, no. 1, pp. 37–58, 2021.
- [26] J. Zhao, X. Zhou, Y. Li, and L. Qian, "Optimizing utility-energy efficiency for the Metaverse over wireless networks under physical layer security," 2023, the full version of this paper, available online at <https://personal.ntu.edu.sg/JunZhao/UEE2023.pdf>.
- [27] D. Niu and B. Li, "An asynchronous fixed-point algorithm for resource sharing with coupled objectives," *IEEE/ACM Transactions on Networking*, vol. 24, no. 5, pp. 2593–2606, 2015.
- [28] L. P. Qian, Y. J. Zhang, and J. Huang, "MAPEL: Achieving global optimality for a non-convex wireless power control problem," *IEEE Transactions on Wireless Communications*, vol. 8, no. 3, pp. 1553–1563, 2009.
- [29] M. Zhao, J.-J. Yu, W.-T. Li, D. Liu, S. Yao, W. Feng, C. She, and T. Q. Quek, "Energy-aware task offloading and resource allocation for time-sensitive services in mobile edge computing systems," *IEEE Transactions on Vehicular Technology*, vol. 70, no. 10, pp. 10 925–10 940, 2021.
- [30] M. Elwady, H.-J. Zepernick, and Y. Hu, "Ssv360: A dataset on subjective quality assessment of 360° videos for standing and seated viewing on an hmd," in *2022 IEEE Conference on Virtual Reality and 3D User Interfaces Abstracts and Workshops (VRW)*, 2022.
- [31] Z. Yang, M. Chen, W. Saad, C. S. Hong, and M. Shikh-Bahaei, "Energy efficient federated learning over wireless communication networks," *IEEE Transactions on Wireless Communications*, vol. 20, no. 3, pp. 1935–1949, 2020.
- [32] X. Huang, G. Dolmans, H. de Groot, and J. R. Long, "Noise and sensitivity in RF envelope detection receivers," *IEEE Transactions on Circuits and Systems II: Express Briefs*, vol. 60, no. 10, pp. 637–641, 2013.